

Analytical Design Equations for Class-E Power Amplifiers

Mustafa Acar, *Student Member, IEEE*, Anne Johan Annema, *Member, IEEE* and Bram Nauta, *Senior Member, IEEE*

Abstract—This paper presents the analytical solution in time domain for the ideal single-ended Class-E Power Amplifier (PA). Based on the analytical solution a coherent non-iterative procedure for choosing the circuit parameters is presented for Class-E PA's with arbitrary duty-cycle and finite dc-feed inductance (e.g. continuously ranging from Class-E with small finite drain inductance to Class-E with RF choke). The obtained analysis results link all known Class-E PA design equations as well as presenting new design equations. The result of the analysis gives more degrees of freedom to designers in their design and optimization by further expanding the design space of Class-E PA.

Index Terms—Power amplifiers, analog circuits, non-linear circuits, circuit theory, circuit analysis.

I. INTRODUCTION

THE Class-E concept has been introduced by Ewing [1] in his doctoral thesis in 1964. Since then many papers analyzing Class-E power amplifier have been published [2]- [24] and many different aspects of Class-E power amplifier (PA) has been analyzed. The published papers can be categorized in two main groups: Class-E PA with RF choke [1]- [11] and Class-E PA with finite dc feed inductor [12]- [24].

The ideal Class-E PA with RF choke has been analyzed and the analytical design equations are given in the literature [2], [3].

An early analysis of Class-E PA with finite dc feed inductance is published by [12] in 1987, followed by e.g. [13] and [14]. The common property of all these papers [22] is that the procedure for obtaining the final circuit design elements is either long, complex and iterative [12], [13] or does not provide much insight into the circuit design or is not analytically exact [14]. The inclusion of some effects such as finite switch-on resistance, finite load quality factor etc. are reported to turn the design procedure into even more lengthy and iterative process [17]- [21].

This paper presents an analytical solution for the ideal Class-E PA, showing the relation between the circuit elements and the input parameters. The solution reveals the existence of infinitely many design equations for the ideal Class-E PA shown in Fig 1b due to freedom in the value of the dc-feed inductor and in the switch duty-cycle. Based on the analytical solution a coherent, non-iterative, procedure for choosing the circuit design elements is presented in this paper.

Manuscript was received July 23, 2006, revised February 5, 2007. This work was supported by STW (The Dutch Technology Foundation).

Mustafa Acar, Anne Johan Annema and Bram Nauta are with IC Design Group of University of Twente (e-mail:m.acar@utwente.nl, a.j.annema@utwente.nl, b.nauta@utwente.nl).

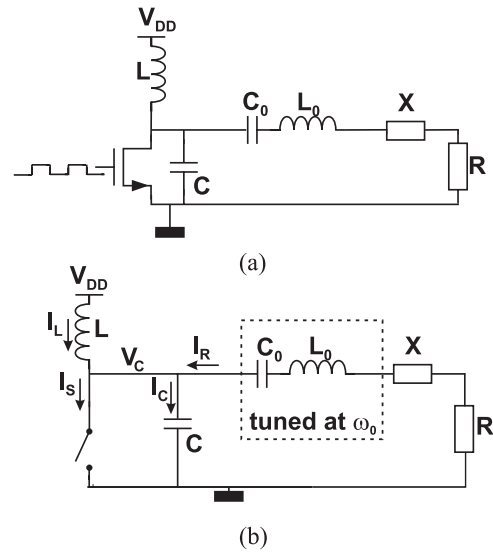


Fig. 1. (a) Single-ended Class-E PA (b) Idealized Model of single-ended Class-E PA

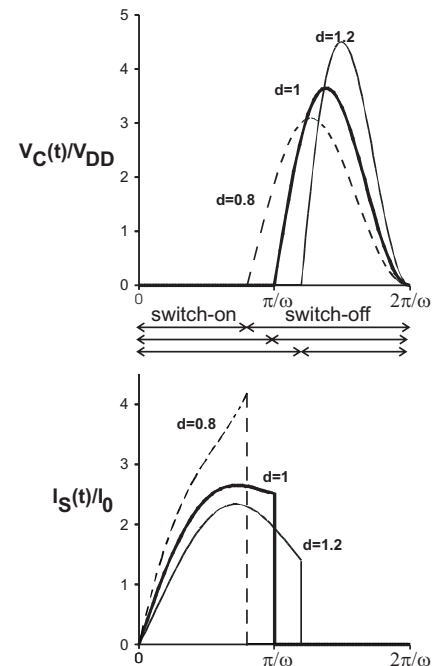


Fig. 2. Normalized switch voltage and switch current of RF choke Class-E PA for $d = 0.8, 1$ and 1.2

The given design equations in [3], [24] and [25] are subsets of the analytical design equation in this paper. The presented analytical design equations expand the design space of Class-E PA, thereby offering much more freedom in the design procedure of a Class-E PA.

The contents of this paper (the present manuscript) significantly extends [27]. In [27], simplified design equations for Class-E PAs are presented and verified experimentally only for a switching duty cycle of 50%. In this paper:

- The analytical design equations for Class-E and their derivation are given.
- An arbitrary switch duty-cycle is allowed which is very important in Class-E PA design [32] whereas only 50% duty-cycle case is considered in [27].
- A design optimization routine for Class-E PA is introduced; this helps design optimal Class-E PA under certain boundary conditions.

The given design equations in [27] are derived from the analytical solution presented in this paper by using curve fitting techniques.

The outline of the paper is as follows. Known Class-E PA design equations are briefly discussed in section II. Well known Class-E PA circuit description, the assumptions in the analysis and the main highlights of the analysis are explained in section III. The Class-E waveforms obtained as a result of the analysis are shown and interpreted in section IV. A number of applications utilizing the infinitely many solutions of Class-E are given in section V. Section VI summarizes the most important findings in this paper.

II. KNOWN DESIGN EQUATIONS

In literature, design equations for Class-E PA can be found that can be used to set the correct values for components in a Class-E PA circuit. For the circuit in Fig 1 different design equations are reported in [3], [24] and [25]. These different design equations form different design sets $K = \{K_L, K_C, K_P, K_X\}$, each consisting of values K_L , K_C , K_P and K_X that relate circuit component values to input parameters such as supply voltage, operating frequency and output power¹. The design sets in [3], [24] and [25] are summarized in Table I ²

The three design sets K given in Table I are specific forms of the Class-E PA shown in Fig 1, with their specific assumptions:

- the design set corresponding to the work in [3] assumes an RF-choke: $L \rightarrow \infty$,
- the parallel circuit Class-E PA in [24] and [23] assumes a zero reactance for X .
- the even harmonic resonant Class-E PA in [25] assumes that $1/\sqrt{LC} = 2n$ where $n = 1, 2, 3, \dots, \infty$.

All of these three subclasses of the Class-E PA (in Fig 1) have their specific advantages and disadvantages. It is reported

¹ L_0 and C_0 seen in Fig 1 can be determined from the chosen quality factor ($Q_L = \omega_0 L_0 / R$) where $\omega_0 = 1/\sqrt{L_0 C_0}$. For the physical meaning of the design set elements K see Appendix I.

²In [3], some symbols (e.g. ψ , B) similar to the design set K elements are used. In order to prevent any confusion we find it wise to show the relation between the given symbols in [3] and this paper $\psi = \tan(K_X)$, $B = K_C/R$.

that the Parallel Circuit Class-E PA [23], [24] and the Even Harmonic Resonant Class-E PA [25] are more size-efficient than the RF-choke Class-E PA [3]. In comparison to RF-choke and Even Harmonic Resonant Class-E the Parallel Circuit Class-E PA allows using higher load resistance, which typically results in a more efficient output matching network and in a possible reduction in the required supply voltage, which might enable the implementation of the Class-E PA in low-voltage technologies. On the other hand, using an RF-choke reduces the sensitivity of the Class-E PA to drain inductance variations.

This paper presents an analytical solution for the design set K for a Class-E PA. This solution shows the existence of not only the aforementioned 3 design sets, but of infinitely many design sets K due to freedom in both the value of dc-feed inductance and in the switch duty-cycle. This yields much more design freedom and much more opportunities to trade advantages and disadvantages of the many design sets K .

III. ANALYSIS OF CLASS-E PA

Analysis of Class-E PAs are already described in literature, see e.g. [3], [12], [23], [24], [26], [21] and [25]. In [3], [24] and [25] an analysis only for one sub-class of Class-E PAs is done. The analysis given in [21], [26] and [12] are based on Laplace transform technique and provide only particular solutions with the presentation of the load network parameters in a table format [23]. In the analysis given in [23], only 50% switch duty-cycle operation is considered and numerical solution techniques are used to derive design equations.

In this paper, a complete analytical derivation is done for ideal Class-E PAs with finite dc-feed inductance and arbitrary duty-cycle. This section presents the analytical derivation of design sets K for Class-E PAs. The complex mathematical results of the current section are simplified and discussed in some detail in sections IV and V.

A. Circuit Description and Assumptions

The circuit schematic of the Class-E PA is given in Figure 1. In the analysis and derivations in this paper a number of assumptions are made:

- the only real power loss in the circuit occurs on load R
- the switch is loss-less with zero on-resistance and infinite off-resistance
- the loaded quality factor (Q_L) of the series resonant circuit (L_0 and C_0) is high enough in order for the output current to be sinusoidal at the switching frequency

Fig. 2 illustrates the switching behavior and the switch definition used in this derivation: in the time interval $0 \leq t < d \cdot \pi/\omega$ the switch is closed and in the time interval $d \cdot \pi/\omega \leq t < 2\pi/\omega$ it is opened. This switching action repeats itself with a period of $2\pi/\omega$. Note that the chosen value of d determines the switch duty-cycle. For example, $d = 1$ corresponds to conventional 50% switch duty-cycle operation.

In order not to have any switching losses it is necessary to satisfy the following well-known Class-E conditions (1) and

TABLE I
KNOWN EXPLICIT DESIGN EQUATIONS FOR CLASS-E

K	RF-choke [3]	Parallel-Circuit [24]	Even Harmonic Resonant [25]
$K_L = \omega L/R$	$\rightarrow \infty$	0.732	3.534
$K_C = \omega CR$	0.1836	0.685	0.071
$K_P = P_{OUT}R/V_{DD}^2$	0.5768	1.365	0.056
$K_X = X/R$	1.152	0	-4.903

(2) [2], [3]:

$$V_C(2\pi/\omega) = 0 \quad (1)$$

$$\left. \frac{dV_C(t)}{dt} \right|_{t=2\pi/\omega} = 0 \quad (2)$$

B. Circuit Analysis

Two fundamental boundary conditions (e.g. continuity of the capacitor voltage and the continuity of the inductor current) are used together with the Class-E conditions ((1) and (2)) in order to solve the relation between the input parameters and the circuit element values in Class-E PAs.

In the analysis, the current into the load, $I_R(t)$, is assumed to be sinusoidal. Note that theoretically this occurs only for infinite Q of the series resonant network consisting of L_0 and C_0 . It is however a widely used assumption that simplifies analysis considerably:

$$I_R(t) = I_R \sin(\omega t + \varphi) \quad (3)$$

In the time interval $0 < t < d \cdot \pi/\omega$, the switch is closed and hence the capacitance voltage $V_C(t) = 0$ and the current through the capacitance $I_C(t) = C \frac{dV_C(t)}{dt} = 0$. In this time interval, the switch current $I_S(t)$ is

$$\begin{aligned} I_S(t) &= I_L(t) + I_R(t) \\ &= \frac{V_{DD}}{L}t + I_L(0) + I_R \sin(\omega t + \varphi) \end{aligned} \quad (4)$$

$$\text{where } I_L(0) = -I_R \sin(\varphi)$$

In the time interval $d \cdot \pi/\omega < t < 2\pi/\omega$, the switch is opened. Then, in the Class-E PA the current through capacitance C is

$$\begin{aligned} I_C(t) &= \frac{1}{L} \int_{d\pi/\omega}^t (V_{DD} - V_C(t)) dt + \\ &I_L \left(\frac{d\pi}{\omega} \right) + I_R(t) \end{aligned} \quad (5)$$

Relation (5) can be re-arranged in the form of a linear, nonhomogeneous, second-order differential equation

$$LC \frac{d^2 V_C(t)}{dt^2} + V_C(t) - V_{DD} - \omega L I_R \cos(\omega t + \varphi) = 0 \quad (6)$$

which has as solution

$$V_C(t) = C_1 \cos(q\omega t) + C_2 \sin(q\omega t) + V_{DD} - \frac{q^2}{1-q^2} p V_{DD} \cos(\omega t + \varphi) \quad (7)$$

$$\text{where } q = \frac{1}{\omega \sqrt{LC}} \quad (8)$$

$$p = \omega L I_R / V_{DD} \quad (9)$$

$$C_1 = \left\{ \frac{q^2 \cos(2q\pi) \cos(\varphi)}{1-q^2} p + \right. \quad (10)$$

$$\left. \frac{\sin(2q\pi) q \sin(\varphi)}{1-q^2} p - \cos(2q\pi) \right\} V_{DD}$$

$$C_2 = \left\{ \frac{\sin(2q\pi) q^2 \cos(\varphi)}{1-q^2} p - \right. \quad (11)$$

$$\left. \frac{q \cos(2q\pi) \sin(\varphi)}{1-q^2} p - \sin(2q\pi) \right\} V_{DD}$$

The coefficients C_1 and C_2 follow from the Class-E equations (1) and (2). It follows from (4) and (7) that $V_C(t)$ and $I_S(t)$ can be expressed in terms of V_{DD} and ω only if d , q , p and φ are known. In Appendix I, the physical meaning of d , q and p are explained. The derivation of these four parameters is the next step in the derivation of the Class-E design equations.

To derive expressions for the four unknowns so far, d , q , p and φ initial off-state conditions: $V_C(d\pi/\omega) = 0$ and $I_L(d\pi/\omega) = V_{DD}d\pi/(\omega L) - I_R \sin(\varphi)$ can be used.

The following two non-linear relations for φ , p , q and d follow from the initial off state conditions. These two relations can be used to solve φ and p analytically in terms of q and d which yields, together with (7), (4) the solution of any Class-E PA. Therefore, here q and d are chosen as free design variables. In theory, q can take any positive real value and d can take any real value³ in the range $0 < d < 2$. The two relations for φ , p , q and d are:

$$f_1(p, \varphi, q, d) = p \left(a_1(q, d) \sin(\varphi) - b_1(q, d) \cos(\varphi) \right) - c_1(q, d) = 0 \quad (12)$$

$$f_2(p, \varphi, q, d) = p \left(a_2(q, d) \sin(\varphi) - b_2(q, d) \cos(\varphi) \right) - c_2(q, d) = 0 \quad (13)$$

The functions $a_1(q, d) \dots c_2(q, d)$ and the details of the analytical solution for p and φ are given in the Appendix II.

³In practical designs, the useful range of both q and d are limited as will be shown later in this paper.

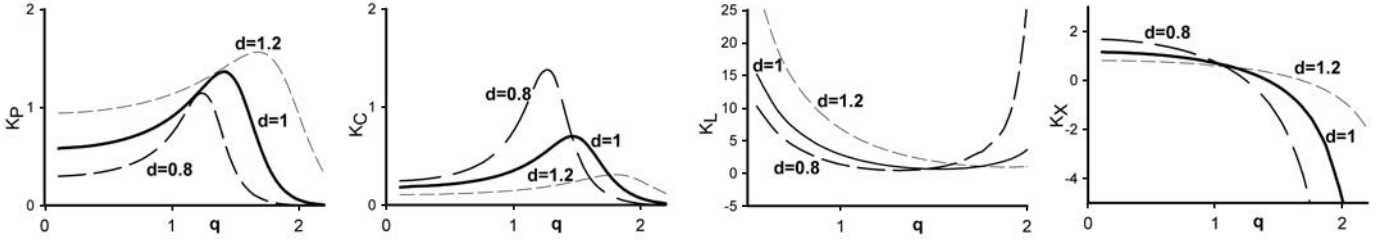


Fig. 3. Elements of the design set $K_P(q), K_C(q), K_L(q), K_X(q)$ as a function of q for $d = 0.8, 1$ and $d = 1.2$

C. Design sets for Class-E operation

The mathematical derivation of the existence of infinitely many solutions due to freedom in the value of dc-feed inductor and in the switch duty-cycle leading to true Class-E operation can be simplified considerably, yielding an easy-to-use design procedure for Class-E PAs. In the previous subsection, it was mentioned that p and φ both can be solved as a function of q and d ; the resulting relations are shown in Fig 4. Using the relations for φ, p, q and d design set $K = \{K_L, K_C, K_P, K_X\}$ can readily be derived.

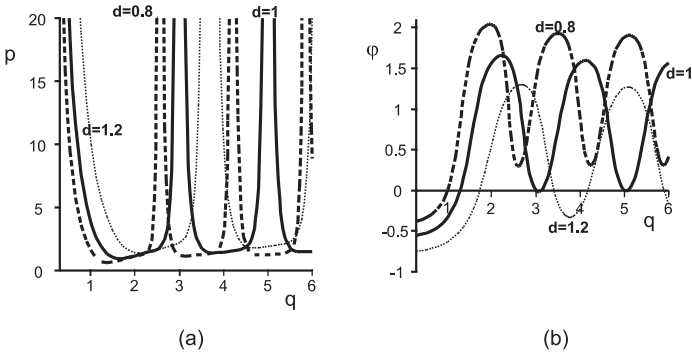


Fig. 4. (a) $p(q, d)$ and (b) $\varphi(q, d)$ as a function of q for $d = 0.8, 1, 1.2$

K_L : The expression for K_L can be derived by using the fact that (with the assumption of an ideal switch) the conversion efficiency from DC power to AC power is 100%:

$$I_R^2 \frac{R}{2} = I_0 V_{DD} \quad (14)$$

In this relation, I_0 is the average supply current:

$$\begin{aligned} I_0 &= \frac{\omega}{2\pi} \int_0^{2\pi/\omega} I_S(t) dt \\ &= I_R \left(\frac{(\pi d)^2}{4p} - \frac{d}{2} \sin(\varphi) - \frac{\cos(d\pi + \varphi)}{2\pi} + \frac{\cos(\varphi)}{2\pi} \right) \end{aligned} \quad (15)$$

Substitution of (15) and (9) in (14) yields

$$K_L(q, d) = \frac{p}{\frac{d^2 \pi}{2p} - 2 \cos(d\pi + \varphi) + 2d\pi \sin(\varphi) + 4 \cos(\varphi)} \quad (16)$$

Since p and φ both are functions of q and d as given in the Appendix II and plotted in Fig 4, $K_L(q)$ is a function of e.g. only q and d .

K_C : K_C follows directly from (8) and (16):

$$K_C(q, d) = \frac{1}{q^2 K_L(q, d)} \quad (17)$$

K_P : An expression for K_P as a function of p and q can easily be found using $I_R = \sqrt{2P_{OUT}/R}$ and (9):

$$K_P(q, d) = \frac{1}{2} \frac{p^2}{K_L(q, d)^2} \quad (18)$$

K_X : An analytical expression for K_X can be derived using two fundamental quadrature Fourier components of $V_C(t)$. The analytical expression for $K_X(q, d)$ in terms of q and d is given in Appendix II.

$$V_R = \frac{1}{\pi} \int_0^{2\pi/\omega} V_C(t) \sin(\omega t + \varphi) dt$$

$$V_X = \frac{1}{\pi} \int_0^{2\pi/\omega} V_C(t) \cos(\omega t + \varphi) dt$$

$$K_X(q, d) = \frac{V_X}{V_R} \quad (19)$$

The values for $K_L(q, d), K_C(q, d), K_P(q, d)$ and $K_X(q, d)$ are plotted in Fig. 3 as a function of q for $d = 0.8, 1$ and 1.2 . Fig. 3 shows that all the elements of the design set K depend very much on both q and d . For example, the maximum value of K_C for $d = 0.8$ can be about 4.2 times higher than the maximum value of K_C for $d = 1.2$; allowing using wider transistors⁴. Besides, the peak value of the switch voltage ($V_C(t)$) for $d = 0.8$ is observed to be smaller than that for $d = 1.2$; which is an important feature for Class-E PA design in technologies with low break-down voltages.

In Fig.5, normalized output power ($U = \frac{P_{OUT}}{I_{MAX} V_{MAX}}$) is given as a function of q for $d = 0.8, 1$ and 1.2 . Fig.5 shows

⁴Generally, in Class-E PA design the parasitic output capacitance of the switch (transistor) should be smaller than $C = K_C/(\omega R)$; implying that higher K_C allows wider transistors which increases the drain efficiency due to the associated lower switch on-resistance.

that U is a strong function of both q and d ; U is maximum for $d = 1$.

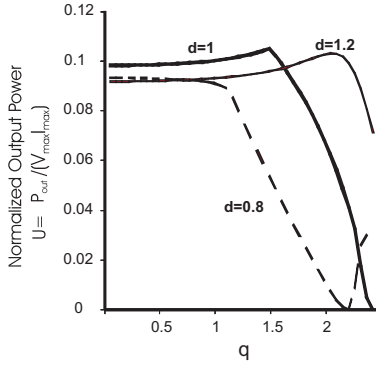


Fig. 5. Normalized Output Power as a function of q for $d = 0.8, 1$ and 1.2

IV. WAVEFORMS

Section III showed that the design set is a function of q and d therefore, there exist infinitely many Class-E realizations for a chosen value of d . Although the switch voltage waveforms of all these Class-E realizations satisfy (1) and (2), the Class-E waveforms for different design sets are different. The Class-E waveforms and the implications on Class-E design are discussed in this section.

A. Achievable Waveforms

For different values of q and d , the Class-E waveforms exhibit significantly different peak voltage and peak current values, having their own pros and cons in circuit design. Therefore, investigation of Class-E waveforms is important from an application point of view. Implementing a Class-E PA using a single transistor, as in Fig 1a, the following properties of Class-E waveform are important:

- the peak value of the switch voltage should be sufficiently low not to exceed the breakdown voltage limits of the transistor.
- the value of the switch current at turn-off moment should be sufficiently low when the switch (transistor) is driven by a sinusoidal driving signal⁵.
- the rms value of the switch current⁶, the inductor (L) current, the capacitor (C) current and the load current should be low to minimize resistive power losses.

As mentioned, Fig 2 shows that the waveform of the switch voltage and the current strongly depend on d . For $d = 0.8$, the peak value of normalized switch voltage is about 30% lower than the peak value of switch voltage for $d = 1.2$. However, it should also be noted that both the maximum value of the switch current and the value of the switch current at the turn-off moment are much higher for $d = 0.8$ than for $d = 1.2$.

⁵For sinusoidal driving signals of the switch (transistor) it is difficult to provide high peak values of the switch current when the input driving signal is going to zero [23].

⁶The on-resistance of the switch (transistor) is usually dominant over other resistive losses.

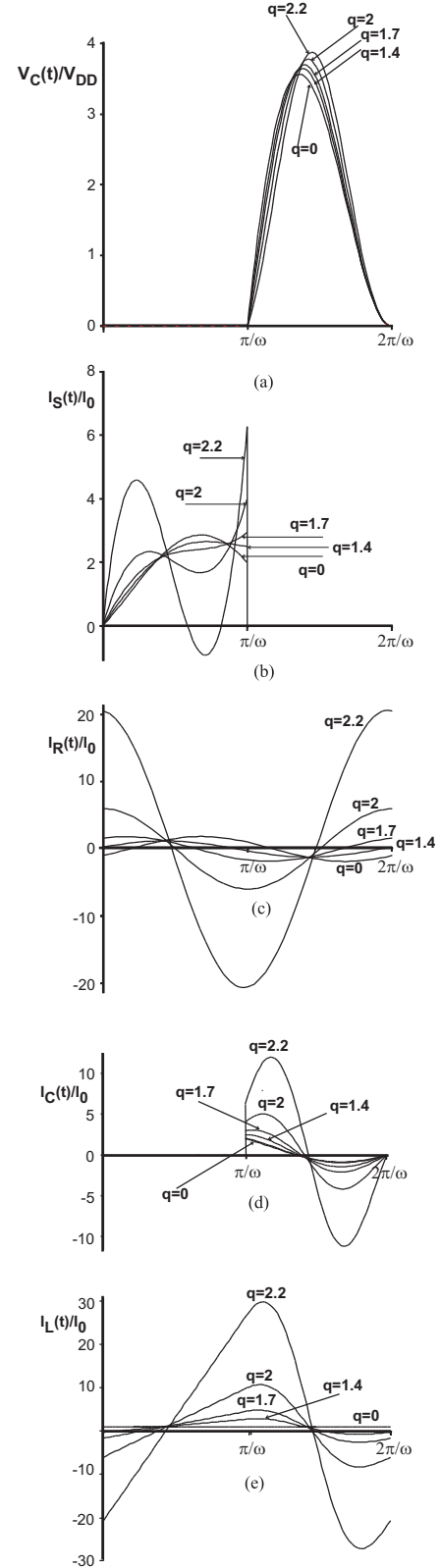


Fig. 6. Normalized (a) switch voltage, (b) switch current (c) load current (d) capacitor (C) current (e) inductor (L) current for different values of q for $d = 1$

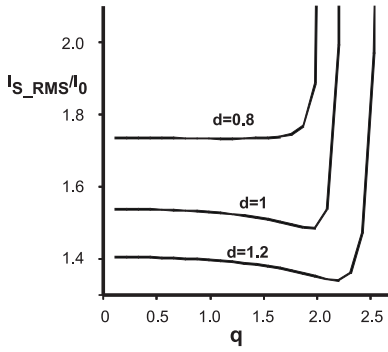


Fig. 7. RMS value of the normalized switch current I_S/I_0 as a function of q for $d = 0.8, 1$ and 1.2

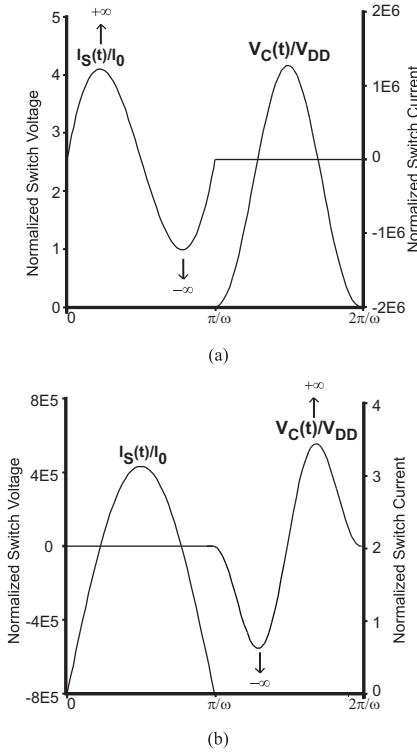


Fig. 8. Normalized (a) switch voltage and switch current for $q = 2.422$, (b) switch voltage and switch current for $q = 3$. For both (a) and (b) $d = 1$ is assumed

Fig 6 shows a number of normalized signal waveforms in the Class-E PA as a function of time for different values of q for $d = 1$. In the figure, the switch voltage is normalized with respect to the supply voltage; the switch current, the load current, the capacitor (C) current and the inductor (L) current are normalized with respect to the dc current (I_0).

As q approaches to 2.2 the peak value of the normalized switch voltage increases from 3.56 to (approximately) 4. Fig 6b shows that for high values of q the switch current, at the moment the switch is opened, increases. Fig 6d and Fig 6e show that the rms current in the capacitor (C) and inductor also increase rapidly with increasing q .

The relation between q and the normalized load current shows a different behavior than that for the capacitor and the inductor current. The lowest rms value of the normalized load current occurs for $q \approx 1.4$.

The rms value of the normalized switch current is shown in Fig 7 as a function of q . Fig 7 shows that from $q = 0$ to $q = 2$ the rms value of the normalized switch current decreases monotonically; from $q = 2$ to $q = 2.2$ the rms value of the normalized switch current increases.

It can be concluded from the results obtained above that there is no value of q that can satisfy all the four points of the "wish list" above at the same time. However, depending on the importance of design criteria a reasonable value of q can be selected.

B. Extreme Waveforms

In the infinitely many Class-E solutions, some are very useful while others appear to be quite impractical because of their extreme waveform behavior. This section discusses the (regions of) most extreme behavior; for simplicity reasons $d = 1$ assumed. This value corresponds to conventional 50% switch duty-cycle. It was shown in this paper that any q -value corresponds to a specific Class-E solution. Extreme behavior occurs for values of q where either

$$1) p(q, d = 1) \rightarrow \infty, \text{ resulting in } \varphi(q, d = 1) = 0$$

The design set K for this condition is

$$\{K_L \rightarrow \infty, K_C = 0, K_P = 0, K_X \rightarrow -\infty\}$$

$$2) \varphi(q, d = 1) = \pi/2, \text{ corresponding to } p(q, d = 1) = \pi/2.$$

The design set K for this condition is

$$\{K_L \rightarrow \infty, K_C = 0, K_P = \text{finite}, K_X \rightarrow -\infty\}$$

It can be shown that both of these situations occur once in every range $2n < q \leq 2n + 1$ where $n = 1, 2, 3, \dots$. Note that the first extreme Class-E PA has zero output power, while the second one has non-zero output power.

For the range $2 < q \leq 3$ the extreme behavior occurs for $q = 2.422$ and $q = 3$. Fig 8 shows the normalized voltage and the current for these two cases. Fig 8a shows that the peak value of the normalized switch current, for $q = 2.422$, approaches to $\pm\infty$ while the peak value of the normalized voltage reaches to 4. Fig 8b shows the same voltage and current for the case that $q = 3$: the peak value of the voltage reaches to $\pm\infty$ whereas the peak value of the current is around 3.5.

In the design of Class-E PA, design sets K corresponding to extreme Class-E behavior should be avoided in order not to encounter infinitely high voltages or currents. Note that while only distinct q -values result in true extreme behavior, a small q -region around the distinct values result in impractical Class-E behavior.

V. DESIGN OPTIMIZATION

In this section, useful examples are given to help engineers in designing Class-E power amplifiers. The simplified versions of the analytical equations for only 50% switch-duty cycle operation given in this section allow the designers to design Class-E PAs without the need to use the analytical solution. However, by using the analytical solution, it is quite straightforward to derive simple design equations for arbitrary switch duty-cycle operation.

Section IV-B discussed Class-E realizations with infinite currents or voltages; these infinitely large signals make it impossible to implement these Class-E PAs in any technology. However, also Class-E realizations with finite signals may be not feasible because of technology limits. This section discusses also practical, technology related, limitations to Class-E realizations. The technology-related limitations taken into account in this section are

- the breakdown limits of the active device (the switch), which sets the maximum value for V_{DD} ,
- the minimum value of the parasitic capacitance C , which is determined by the output capacitance of the active device,
- the minimum value of the load resistance R , which determines (with the quality factor of the components in the output matching network) the maximum acceptable losses of the output matching network,
- the parasitic inductances present in the circuit, which set the lowest value of inductors that can be used in the Class-E PA, and
- the tolerable physical sizes of passives, which sets an upper bound on the quality factor and maximum value of the reactive components.

Clearly these boundary conditions narrow the useful range of q , by excluding certain regions of q for a chosen d . The analytical design equations in this paper enable the selection of the best performing true Class-E PA inside the remaining design space. A simplified approach as well as an example are provided in this section.

A. Simplified Design Equations

The exact analytical expressions are somewhat hard to handle. However, using the total design space for Class-E PAs typically is not very useful. A restriction to values of q that result in reasonable power output for manageable component values and quality factors enables a significant simplification for a chosen value of d .

In this section $d = 1$ which corresponds to the traditional 50% duty-cycle operation; clearly depending on the performance benefits different values of d can also be chosen and curve fitted by using the analytical solution given in this paper. As explained, the switch duty-cycle has important impact on the performance of Class-E PAs especially at high frequency of operation (> 1 GHz) [32]. The design space for which output power and component properties are very well suited for today's applications and technologies corresponds roughly to the q -range $0 < q < 1.9$ for $d = 1$.

For this q -range, the exact analytical expressions can easily be fitted to (four) simple polynomial expressions, each covering a part of the range.

- 1) for the range $0 < q < 0.6$ and $d = 1$
the design elements K_C , K_P , K_X don't change significantly and $K_L > 10$. Therefore in this range the design equations for the RF-choke Class-E PA [3], see Table I, can be used.
- 2) for the range $0.6 < q < 1$ and $d = 1$
the exact results can be fitted reasonably well using

second order polynomials. The resulting (fitted) design set relations are shown in Table II.

TABLE II
DESIGN SET FOR ($0.6 < q < 1$)

$$\begin{aligned} K_L(q, d = 1) &= 44.93q^2 - 94.32q + 52.46 \\ K_C(q, d = 1) &= 0.426q^2 - 0.379q + 0.3 \\ K_P(q, d = 1) &= 0.74q^2 - 0.6q + 0.76 \\ K_X(q, d = 1) &= -0.73q^2 + 0.411q + 1.03 \end{aligned}$$

- 3) for the range $1 < q < 1.65$ and $d = 1$
a reasonably accurate fit is presented in Table III.

TABLE III
DESIGN SET FOR ($1 < q < 1.65$)

$$\begin{aligned} K_L(q, d = 1) &= 8.085q^2 - 24.53q + 19.23 \\ K_C(q, d = 1) &= -6.97q^3 + 25.93q^2 - 31.071q + 12.48 \\ K_P(q, d = 1) &= -11.90q^3 + 42.753q^2 - 49.63q + 19.70 \\ K_X(q, d = 1) &= -2.9q^3 + 8.8q^2 - 10.2q + 5.02 \end{aligned}$$

- 4) for the range $1.65 < q < 1.9$ and $d = 1$
a reasonably accurate fit is presented in Table IV.

TABLE IV
DESIGN SET FOR ($1.65 < q < 1.9$)

$$\begin{aligned} K_L(q, d = 1) &= 16.17q^2 - 52.26q + 42.94 \\ K_C(q, d = 1) &= 2.55q^2 - 10.53q + 10.92 \\ K_P(q, d = 1) &= 6.25q^2 - 24.73q + 24.56 \\ K_X(q, d = 1) &= -16.84q^2 + 51.38q - 39.83 \end{aligned}$$

The difference between the fitted design equations and the exact analytical relations is in the order of $\approx 2\%$. The difference can be further reduced by curve fitting with higher order of polynomials.

In [22], similar simplified design equations for Class-E PA is obtained by applying polynomial curve-fitting techniques on the interpolated numerical solutions for the set K . The technique used in [22] depends on numerical solution methods and the design equations given don't take into account capacitive values for X .

B. Optimum design sets

The choice for using one of the infinitely many possible design equations depends on the boundary conditions imposed by the operating conditions and by the technology. For example, the maximum output power for given R and V_{DD} is obtained for $q = 1.412$ where $K_P(q, d = 1)$ reaches its maximum. The corresponding design set K was already published in e.g. [24] through numerical solution methods:

Similarly, for given R and C the maximum operation frequency is reached at $q = 1.468$ where $K_C(q, d = 1)$ reaches its maximum. The design set K for maximum operation frequency is given in Table VI.

The design equations given in Table IV for $1.65 < q < 1.9$ is very useful in the design of integrated low power Class-E PAs. Mainly, there are two design challenges for low power

TABLE V
DESIGN SET FOR MAXIMUM OUTPUT POWER

$K_L = 0.732$
$K_C = 0.685$
$K_P = 1.365$
$K_X = 0$

TABLE VI
DESIGN SET FOR MAXIMUM OPERATION FREQUENCY

$K_L = 0.661$
$K_C = 0.702$
$K_P = 1.332$
$K_X = -0.159$

Class-E (e.g. Biomedical applications or Low Power Sensors Systems etc. [28], [29]) PAs;

- Low output power with high power-added efficiency (PAE)
- Small size

Two conventional approaches seen in the literature to design low power PAs are either to lower supply voltage [28] or to use a matching network to step-up the 50Ω antenna impedance to higher values in order to lower the output power. The former solution may require DC-DC converter like additional circuits increasing size, design complexity and cost while the latter solution may decrease the efficiency due to the loss in the matching network depending on the required impedance transformation ratio [30].

Using the design set in Table IV for $1.65 < q < 1.9$ will help to decrease the output power without the need to resort to methods such as decreasing the supply voltage or the load resistance. Since $P_{OUT} = K_P V_{DD}^2 / R$, decreasing K_P nearly to zero as q approaches to 1.9 helps to design low-power Class-E PAs. Besides, the decrease in the rms value of the switch current for $1.65 < q < 1.9$ as seen in Fig 7 helps decreasing the power loss on the switch; increasing PAE.

Clearly many more optimum design sets can be derived, each optimizing for some operating condition, for some component value or for some (in)sensitivity.

C. An Optimization Routine

In the design phase of a Class-E PA, all the component values must be found for some target operating conditions. These operating conditions are in terms of (angular) frequency, output power and supply voltage. In this section, all the component values and operating conditions are grouped into a set P . For true Class-E operation the component values and operating conditions are linked together via the design set $K(q, d)$. Note that X may be inductive or capacitive, depending on the sign of $K_X(q, d)$ or on the value of q : for example for $d = 1$ if $q < 1.412$ then $X = \omega L_X$ while for $q > 1.412$ $X = -\frac{1}{\omega C_X}$.

$$\begin{aligned} K &= \{K_C(q, d), K_L(q, d), K_P(q, d), K_X(q, d)\} \\ &= \left\{ \omega C R, \frac{\omega L}{R}, \frac{P_{OUT} R}{V_{DD}^2}, \frac{X}{R} \right\} \\ P &= \{L, R, C, P_{OUT}, V_{DD}^2, \omega, X\} \end{aligned}$$

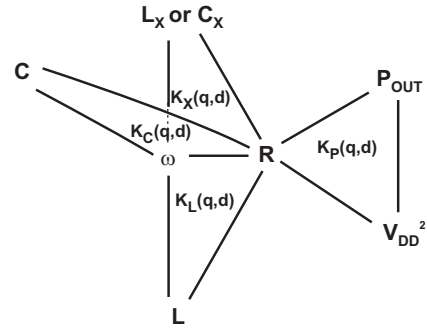


Fig. 9. Drawing to show the relations between the elements of the design set K

Inspection of the relations for the elements in K , shows that every element in K links three elements of P together; Fig 9 shows these relations graphically. In Fig 9, each circuit element or input parameter is placed in the corners of a triangle and the related design set element is shown in the inner part of the triangle. In the triangles for $K_C(q, d)$, $K_L(q, d)$, $K_X(q, d)$ two elements are shared by the other triangles, whereas in $K_P(q, d)$ only one element R is shared. Therefore, either V_{DD} or P_{OUT} must be known in order to be able to make a uniquely defined Class-E PA design. At the same time the set P turns into a smaller set $P' = \left\{ L, R, C, \frac{P_{OUT}}{V_{DD}^2}, \omega, X \right\}$.

It can be shown with the help of Fig 9 that if any two elements of the set P' are known, the rest of the elements can be expressed in terms of q . For a chosen d the selection of a proper q , a q -value that satisfies possible boundary conditions in terms of e.g. component values, then fixes the total design. The next subsection presents two optimization examples.

D. Design Examples

This section presents two applications of the analytical design equations to the circuit design of Class-E PAs. The design flows of these two examples are given in Fig 10 and Fig 11. In each of the flows two elements from P' are assumed to be known a priori. The remaining variables then can be expressed in terms of q for a chosen value of d . A suitable q value that satisfies some particular boundary conditions can easily be selected from the graph, after which the Class-E design is completed.

The aim in the first design example in Fig 10 is to demonstrate a procedure to find the maximum output power that can be obtained from a discrete transistor when it is designed as a Class-E PA. In this procedure, a discrete transistor with a certain maximum drain current ($I_{max} = 1$ A) and drain voltage ($V_{max} = 1$ V) is assumed to be used for Class-E PA design. For power amplifier designers it is very important to know in advance how much power can be obtained from a discrete transistor. The maximum output power can be determined from the transistor utilization factor (normalized output power), as $P_{OUT}(q, d) = U(q, d) I_{max} V_{max}$. For the chosen duty-cycle a range of q can be chosen for the desired P_{OUT} level. For example, for $P_{OUT} > 0.08$ W (shown with red arrow in Fig 10) q is restricted to the range $0 < q < 1.2$ for $d = 0.8$.

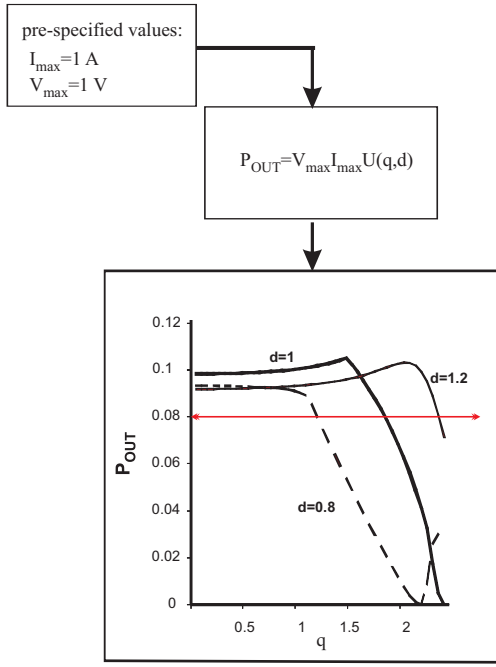


Fig. 10. Design-1, Class-E Design Optimization Flow Chart

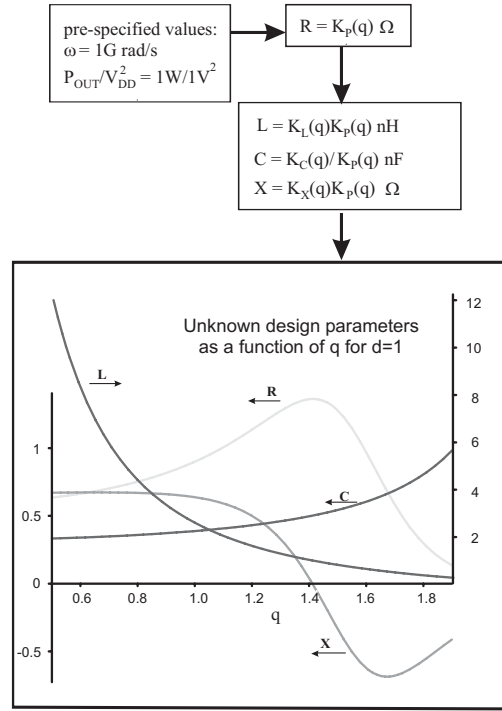


Fig. 11. Design-2, Class-E Design Optimization Flow Chart

In the second design given in Fig 11, the goal is to design a Class-E power amplifier with the angular frequency ω , output power and supply voltage are as $\omega = 1 \text{ G rad/s}$, $P_{OUT} = 1 \text{ W}$ and $V_{DD} = 1 \text{ V}$ respectively. By using the design set K the other design parameters are obtained in terms of q and plotted in Fig 11. Choosing a value for q finalizes the design. In this example $d = 1$ is assumed. A suitable q depending on the boundary conditions for the rest of the design variables can be chosen to determine all the design parameters. For example, the maximum load resistance $R = 1.35 \Omega$ is obtained for $q = 1.412$ for which the inductor (L), the capacitor (C) and the excess reactance (X) are 0.99 nH , 0.51 nF and 0Ω respectively. Depending on the chosen value of Q_L the value of L_0 and C_0 can easily be determined and the design is finalized.

As it is seen in both of the design examples the optimization routine makes the design process very straightforward. In fact, once any two elements of the set $P' = \{L, R, C, \frac{P_{OUT}}{V_{DD}^2}, \omega, X\}$ are given and the design set K is known in terms of q all the circuit element values can easily be calculated without the need to understand the details of the derivation procedure.

The two design examples in Fig 10 and Fig 11 clearly illustrate that optima are heavily dependent on both the property to optimize and on the a priori fixed values.

VI. CONCLUSION

This paper presents an analytical solution in time domain for the Class-E PA by taking into account both the switch duty-cycle and the finite dc-feed inductance. The analytical solution show the existence of infinitely many design equations for Class-E PAs due to the freedom both in the value of switch duty-cycle and in the dc-feed inductance.

By using this analytical solution a non-iterative coherent procedure for choosing the circuit design parameters for Class-E PAs is presented. The well-known Class-E design equations in literature are specific solutions out of the total Class-E design space.

By means of the analytical design equations the waveform characteristics of Class-E PAs are investigated and a number of trade-offs is discussed. To enable easy Class-E design, a (non-iterative) design procedure is given that enables optimization of the Class-E PA under e.g. boundary conditions on circuit element values and operating conditions. Within this method the extra degrees of freedom associated with the continuum of different Class-E design equations is exchanged for optimization.

APPENDIX I

In this section, a rough description of the physical meanings of the elements of the design set $K = \{K_L, K_C, K_X, K_P\}$ and the variables d, q, p are given.

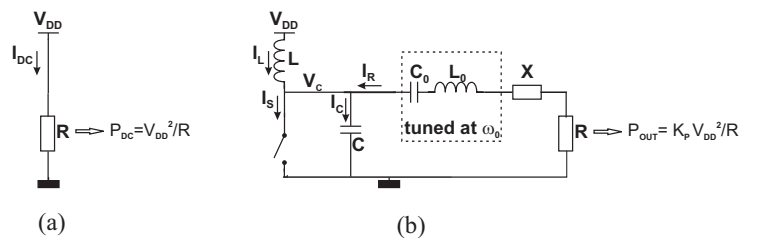


Fig. 12. (a) Supply Voltage-Resistive Load (b) Idealized Class-E PA

$$p_1(q, d) = \frac{\sqrt{\left(b_2(q, d)^2 + a_2(q, d)^2\right)\left(c_1(q, d)^2 + c_2(q, d)^2\right) - 2\left(a_1(q, d)a_2(q, d) + b_2(q, d)b_1(q, d)\right)c_2(q, d)c_1(q, d)}}{-a_1(q, d)b_2(q, d) + b_1(q, d)a_2(q, d)} \quad (20)$$

A. Physical Meaning of the Design Set K

The design set (K) elements $K_L = \frac{\omega L}{R}$, $K_C = \omega CR$, $K_X = \frac{X}{R}$ are defined as the impedance of the passive elements at the operation frequency to the load R . The physical meaning of the term K_P can be explained by using Fig. 12.

An ideal Class-E power amplifier can convert DC power to AC power with 100% drain efficiency. The DC power that can be obtained from a DC source (V_{DD}) for a resistive load of R is $P_{DC} = \frac{V_{DD}^2}{R}$, Fig. 12a. For the Class-E PA in Fig. 12b the output power is K_P times higher than the power in Fig. 12a. Therefore, the term K_P can be named as "power scaling factor".

B. Physical Meaning of the variables d , q and p

The variable d directly determines the switch duty-cycle= (50 d)%. For example, $d = 1$ corresponds to 50% switch duty-cycle.

The variable $q = \frac{1}{\omega\sqrt{LC}} = \frac{\omega_p}{\omega}$. Here ω_p is the angular frequency to which $L-C$ parallel network is tuned. Therefore, physically q can be seen as the ratio of the parallel tuned frequency (ω_p) to operation frequency (ω).

From a physical point of view, the variable $p = \frac{\omega LI_R}{V_{DD}} = \frac{\omega L}{V_{DD} I_R}$ corresponds to the ratio of the impedance of L at the operation frequency (ω) to the resistance $\frac{V_{DD}}{I_R}$ that the amplifier shows to the power supply (V_{DD}) for the fundamental load current.

APPENDIX II

In this appendix, the analytical solution for the variables p and φ are given as well as the analytical solution for the design set (K) element K_X .

A. Analytical Solution for the Set of Equations

For proper Class-E operation two equations, (21)-(22), were derived. In this appendix the analytical solution for this set of equations is given, leading to the generalized design equation continuum for Class-E PAs.

$$f_1(p, \varphi, q, d) = p\left(a_1(q, d) \sin(\varphi) - b_1(q, d) \cos(\varphi)\right) - c_1(q, d) = 0 \quad (21)$$

$$f_2(p, \varphi, q, d) = p\left(a_2(q, d) \sin(\varphi) - b_2(q, d) \cos(\varphi)\right) - c_2(q, d) = 0 \quad (22)$$

Two out of the four variables can be expressed in terms of q and d using (21)-(22). The solution set is

$\left\{\left(p_1(q, d), \varphi_1(q, d)\right), \left(p_2(q, d), \varphi_2(q, d)\right)\right\}$ where the elements are given by (20)-(25).

$$p_2(q, d) = -p_1(q, d) \quad (23)$$

$$\varphi_1(q, d) = \arctan\left(-b_2(q, d)c_1(q, d) + c_2(q, d)b_1(q, d), -a_1(q, d)c_2(q, d) + c_1(q, d)a_2(q, d)\right) \quad (24)$$

$$\varphi_2(q, d) = \arctan\left(b_2(q, d)c_1(q, d) - c_2(q, d)b_1(q, d), a_1(q, d)c_2(q, d) - c_1(q, d)a_2(q, d)\right) \quad (25)$$

The definition for $\arctan(y, x)$: the angle between the x-axis and the line from (0,0) to (x,y)

$$a_1(q, d) = -1 - \frac{1}{q} \left\{ -\frac{\sin(2q\pi)q \sin(qd\pi)}{1-q^2} + \frac{q \cos(d\pi)}{1-q^2} - \frac{q \cos(2q\pi) \cos(qd\pi)}{1-q^2} \right\} + \cos(d\pi)$$

$$b_1(q, d) = -\frac{1}{q} \left\{ -\frac{q^2 \cos(2q\pi) \sin(qd\pi)}{1-q^2} + \frac{q \sin(d\pi)}{1-q^2} + \frac{\sin(2q\pi)q^2 \cos(qd\pi)}{1-q^2} \right\} + \sin(d\pi)$$

$$c_1(q, d) = d\pi - \frac{\cos(2q\pi) \sin(qd\pi) - \sin(2q\pi) \cos(qd\pi)}{q}$$

$$a_2(q, d) = -\left\{ \frac{q \cos(2q\pi) \sin(qd\pi)}{1-q^2} \right\} + \frac{\sin(2q\pi)q \cos(qd\pi)}{1-q^2} + \frac{q^2 \sin(d\pi)}{1-q^2}$$

$$b_2(q, d) = -\frac{q^2 \cos(d\pi)}{1-q^2} + \frac{\sin(2q\pi)q^2 \sin(qd\pi)}{1-q^2} + \frac{q^2 \cos(2q\pi) \cos(qd\pi)}{1-q^2}$$

$$c_2(q, d) = -\sin(2q\pi) \sin(qd\pi) - \cos(2q\pi) \cos(qd\pi) + 1$$

B. Analytical Expression for $K_X(q, d)$

The design set $K_X(q, d)$ can be obtained in terms of q and d . In order to obtain the analytical expression for $K_X(q, d)$ two fundamental quadrature Fourier components of $V_C(t)$ can be used.

$$V_R = \frac{1}{\pi} \int_0^{2\pi/\omega} (V_C(t) \sin(\omega t + \varphi)) dt$$

$$V_X = \frac{1}{\pi} \int_0^{2\pi/\omega} (V_C(t) \cos(\omega t + \varphi)) dt$$

$$K_X(q, d) = \frac{V_X}{V_R} = \frac{x_1 + x_2 + x_3 + x_4}{y_1 + y_2 + y_3 + y_4}$$

where

$$\begin{aligned}
y_1(q, d) &= -\left(-(\cos(d\pi))^2 + 1\right) q^2 (\cos(\varphi))^2 p V_{DD} \\
y_2(q, d) &= -\left\{q^2 \sin(d\pi) \cos(d\pi) \sin(\varphi) p - \right. \\
&\quad q^2 \cos(d\pi) + q^2 - 1 + \cos(d\pi)\} V_{DD} + \\
&\quad \left\{\cos(d\pi) \sin(qd\pi) - q \sin(d\pi) \cos(qd\pi) - \right. \\
&\quad \left. 2 \sin(q\pi) \cos(q\pi)\right\} C_2 + \left\{\cos(d\pi) \cos(qd\pi) \right. \\
&\quad \left. + 1 + q \sin(d\pi) \sin(qd\pi) \right. \\
&\quad \left. - 2 (\cos(q\pi))^2\right\} C_1 \} \cos(\varphi) \\
y_3(q, d) &= -\left\{(-1 + q^2) \sin(d\pi) V_{DD} + \right. \\
&\quad \left\{\left(-1 + 2 (\cos(q\pi))^2 - \cos(d\pi) \cos(qd\pi)\right) q \right. \\
&\quad \left. - \sin(d\pi) \sin(qd\pi)\right\} C_2 + \left\{\cos(d\pi) \sin(qd\pi) \right. \\
&\quad \left. - 2 \sin(q\pi) \cos(q\pi)\right\} q \\
&\quad \left. - \sin(d\pi) \cos(qd\pi)\right\} C_1 \} \sin(\varphi) \\
y_4(q, d) &= -\frac{\left(-1 + (\cos(d\pi))^2\right) q^2 p V_{DD}}{2} \\
x_1(q, d) &= q^2 p V_{DD} \sin(d\pi) \cos(d\pi) (\cos(\varphi))^2 \\
x_2(q, d) &= \left\{(-1 + q^2) \sin(d\pi) V_{DD} + \right. \\
&\quad \left\{-1 + 2 (\cos(q\pi))^2 - \cos(d\pi) \cos(qd\pi)\right\} q \\
&\quad \left. - \sin(d\pi) \sin(qd\pi)\right\} C_2 \\
&\quad + \left\{(\cos(d\pi) \sin(qd\pi) - \sin(2q\pi)) q - \right. \\
&\quad \left. \sin(d\pi) \cos(qd\pi)\right\} C_1 \} \cos(\varphi) \\
x_3(q, d) &= \left\{((-2p + 2p (\cos(d\pi))^2) \cos(\varphi) - 2 + \right. \\
&\quad \left. 2 \cos(d\pi)) q^2 + 2 - 2 \cos(d\pi)\right\} \sin(\varphi) V_{DD} + \\
&\quad \left\{-2 \cos(d\pi) \sin(qd\pi) + 2 q \sin(d\pi) \cos(qd\pi) \right. \\
&\quad \left. + 4 \sin(q\pi) \cos(q\pi)\right\} \sin(\varphi) C_2 + \\
&\quad \left\{-2 q \sin(d\pi) \sin(qd\pi) - 2 \cos(d\pi) \cos(qd\pi) \right. \\
&\quad \left. - 2 + 4 (\cos(q\pi))^2\right\} \sin(\varphi) C_1 \\
x_4(q, d) &= \frac{(q^2 p d\pi - q^2 p \sin(d\pi) \cos(d\pi) - 2 q^2 p \pi) V_{DD}}{2}
\end{aligned}$$

ACKNOWLEDGMENT

The authors would like to thank to Bram Verhoef and Talitha Faber for fruitful discussions.

REFERENCES

- [1] G. D. Ewing, "High-Efficiency Radio-Frequency Power Amplifier" *PhD thesis*, Oregon State University, Corvallis, Oregon, June 1964
- [2] Sokal, N. O.; Sokal, A.D.; "Class E-A new class of high-efficiency tuned single-ended switching power amplifiers" *Solid-State Circuits, IEEE Journal of*, vol. 10, issue 3, pp. 168 - 176, Jun 1975.
- [3] Raab, F.; "Idealized operation of the class E tuned power amplifier" *Circuits and Systems, IEEE Transactions on* Volume 24, Issue 12, Dec 1977 Page(s):725 - 735
- [4] Raab, F. H.; "Effects of circuit variations on the class E tuned power amplifier" *Solid-State Circuits, IEEE Journal of* vol. 13, Issue 2, Apr 1978 Page(s):239 - 247
- [5] Hung-Lung Tu, S.; Toumazou, C.; "Effect of the loaded quality factor on power efficiency for CMOS class-E RF tuned power amplifiers" *Circuits and Systems I: Fundamental Theory and Applications, IEEE Transactions on* [see also *Circuits and Systems I: Regular Papers, IEEE Transactions on*] Volume 46, Issue 5, May 1999 Page(s):628 - 634.
- [6] Kessler, D.J.; Kazimierczuk, M.K.; "Power losses and efficiency of class-E power amplifier at any duty ratio" *Circuits and Systems I: Regular Papers, IEEE Transactions on* [see also *Circuits and Systems I: Fundamental Theory and Applications, IEEE Transactions on*] Volume 51, Issue 9, Sept. 2004 Page(s):1675 - 1689
- [7] Marian K. Kazimierczuk and Krzysztof Puczek "Power-output capability of class E amplifier at any loaded Q and switch duty cycle" *Circuits and Systems, IEEE Transactions on* Volume 36, Issue 8, Aug. 1989 Page(s):1142 - 1143
- [8] M. K. Kazimierczuk and K. Puczek, "Exact analysis of class E tuned power amplifier at any Q and switch duty cycle," *IEEE Trans. Circuits Syst.*, vol. 34, pp. 149158, Feb. 1987.
- [9] M. K. Kazimierczuk, "Effects of the collector current fall time on the class E tuned power amplifier," *IEEE J. Solid-State Circuits*, vol. SC-18, pp. 181193, Apr. 1983.
- [10] Alinikula, P.; "Optimum component values for a lossy Class E power amplifier" *Microwave Symposium Digest, 2003 IEEE MTT-S International* Volume 3, 8-13 June 2003 Page(s):2145 - 2148 vol.3
- [11] J. A. Blanchard and J. S. Yuan, "Effects of collector current exponential decay on power efficiency for class E tuned power amplifier," *IEEE Trans. Circuits Syst. I*, vol. 41, pp. 6972, Jan. 1994.
- [12] Zulinski, R.; Steadman, J.; "Class E Power Amplifiers and Frequency Multipliers with finite DC-Feed Inductance" *Circuits and Systems, IEEE Transactions on* Volume 34, Issue 9, Sep 1987 Page(s):1074 - 1087
- [13] Li, C.-H.; Yam, Y.-O.; "Maximum frequency and optimum performance of class E power amplifiers" *Circuits, Devices and Systems, IEE Proceedings* [see also *IEE Proceedings G- Circuits, Devices and Systems*] Volume 141, Issue 3, June 1994 Page(s):174 - 184
- [14] Choi, D.K.; Long, S.I.; "Finite DC feed inductor in class E power amplifiers-a simplified approach" *Microwave Symposium Digest, 2002 IEEE MTT-S International* Volume 3, 2-7 June 2002 Page(s):1643 - 1646
- [15] Sekiya, H.; Sasase, I.; Mori, S.; "Computation of design values for Class E amplifiers without using waveform equations" *Circuits and Systems I: Fundamental Theory and Applications, IEEE Transactions on* [see also *Circuits and Systems I: Regular Papers, IEEE Transactions on*] Volume 49, Issue 7, July 2002 Page(s):966 - 978
- [16] Reynaert, P.; Mertens, K.L.R.; Steyaert, M.S.J.; "A state-space behavioral model for CMOS class E power amplifiers" *Computer-Aided Design of Integrated Circuits and Systems, IEEE Transactions on* Volume 22, Issue 2, Feb. 2003 Page(s):132 - 138
- [17] Wang, C.; Larson, L.E.; Asbeck, P.M.; "Improved design technique of a microwave class-E power amplifier with finite switching-on resistance" *Radio and Wireless Conference, 2002. RAWCON 2002. IEEE* 11-14 Aug. 2002 Page(s):241 - 244
- [18] Ho, C.K.; Wong, H.; Ma, S.W.; "Approximation of non-zero transistor ON resistance in class-E amplifiers" *Proceedings of the Fifth IEEE International Caracas Conference on* Volume 1, 3-5 Nov. 2004 Page(s):90 - 93
- [19] Mandojana, J.C.; Herman, K.J.; Zulinski, R.E.; "A discrete/continuous time-domain analysis of a generalized class E amplifier" *Circuits and Systems, IEEE Transactions on* Volume 37, Issue 8, Aug. 1990 Page(s):1057 - 1060
- [20] Choi, Y.-B.; Cheng, K.-K.M.; "Generalised frequency-domain analysis of microwave Class-E power amplifiers" *Microwaves, Antennas and Propagation, IEE Proceedings*, Volume 148, Issue 6, Dec. 2001 Page(s):403 - 409
- [21] Avratoglou, C.P.; Voulgaris, N.C.; Ioannidou, F.I.; "Analysis and design of a generalized class E tuned power amplifier" *Circuits and Systems, IEEE Transactions on* Volume 36, Issue 8, Aug. 1989 Page(s):1068 - 1079
- [22] Milosevic, D.; van der Tang, J.; van Roermund, A.; "Explicit design equations for class-E power amplifiers with small DC-feed inductance" *Circuit Theory and Design, 2005. Proceedings of the 2005 European Conference on* Volume 3, 29th August - 1st September 2005 Page(s):101 - 104
- [23] Andrei Grebennikov "Load Network Design Techniques for Class E RF and Microwave Amplifiers" *High Frequency Electronics*, July 2004.
- [24] Grebennikov, A.V.; Jaeger, H.; "Class E with parallel circuit - a new challenge for high-efficiency RF and microwave power amplifiers" *Microwave Symposium Digest, 2002 IEEE MTT-S International* Volume 3, 2-7 June 2002 Page(s):1627 - 1630

- [25] M. Iwadare, S. Mori, and K. Ikeda, "Even Harmonic Resonant Class E Tuned Power Amplifier without RF Choke," *Electronics and Communications in Japan*, Vol. 79, pp. 23-30, Jan. 1996.
- [26] Smith, G.H.; Zulinski, R.E.; "An exact analysis of class E amplifiers with finite DC-feed inductance at any output Q" *Circuits and Systems, IEEE Transactions on* vol. 37, Issue 4, April 1990 pp:530 - 534
- [27] M. Acar, A.J. Annema, B. Nauta "Generalized Design Equations for Class-E Power Amplifiers with Finite DC Feed Inductance" *36th European Microwave Conference, 2006* 10-15 September 2006, Manchester, UK. pp. 1308-1311
- [28] Chee, Y.H.; Rabaey, J.; Niknejad, A.M.; "A class A/B low power amplifier for wireless sensor networks" *Proceedings of International Symposium on Circuits and Systems*, vol. 4, May 2004 pp: 409-412
- [29] Hyoung-Seok Oh; Taeksang Song; Euisik Yoon; Choong-Ki Kim;"A power-efficient injection-locked class-E power amplifier for wireless sensor network" *Microwave and Wireless Components Letters, IEEE [see also IEEE Microwave and Guided Wave Letters* volume 16, Issue 4, April 2006 Page(s):173 - 175
- [30] P. L. D. Abrie, "Design of Impedance-Matching Networks for Radio-Frequency and Microwave Amplifiers". *Norwood, MA: Artech House*, 1985.
- [31] Albulet, M.; Zulinski, R.E.; "Effect of switch duty ratio on the performance of Class E circuits" *Circuits and Systems, 1997. Proceedings of the 40th Midwest Symposium on* Volume 1, 3-6 Aug. 1997 Page(s):99 - 105 vol.1
- [32] Lie, D.Y.C.; Lee, P.; Popp, J.D.; Rowland, J.F.; Ng, H.H.; Yang, A.H.; "The limitations in applying analytic design equations for optimal class E RF power amplifiers design" *VLSI Design, Automation and Test, IEEE* 2005, pp:161 - 164



Bram Nauta was born in Hengelo, The Netherlands, in 1964. In 1987 he received the M.Sc degree (cum laude) in electrical engineering from the University of Twente, Enschede, The Netherlands. In 1991 he received the Ph.D. degree from the same university on the subject of analog CMOS filters for very high frequencies. In 1991 he joined the Mixed-Signal Circuits and Systems Department of Philips Research, Eindhoven the Netherlands, where he worked on high speed AD converters. From 1994 he led a research group in the same department, working on "analog key modules". In 1998 he returned to the University of Twente, as full professor heading the IC Design group in the MESA+ Research Institute and department of Electrical Engineering. His current research interest is analog CMOS circuits for transceivers. Besides, he is also part-time consultant in industry and in 2001 he co-founded Chip Design Works. His Ph.D. thesis was published as a book: Analog CMOS Filters for Very High Frequencies, Boston, MA, Kluwer, 1993. He holds 11 patents in circuit design and he received the "Shell Study Tour Award" for his Ph.D. Work. From 1997-1999 he served as Associate Editor of IEEE Transactions on Circuits and Systems -II; Analog and Digital Signal Processing, and in 1998 he served as Guest Editor for IEEE Journal of Solid-State Circuits. In 2001 he became Associate Editor for IEEE Journal of Solid-State Circuits and he is also member of the technical program committee of ESSCIRC and ISSCC. He is co-recipient of the ISSCC 2002 "Van Vessel Outstanding Paper Award"



Mustafa Acar was born in Gaziantep, Turkey in 1979. He received his B.S degree (honor) from Middle East Technical University and M.S degree (high honor) in microelectronics from University of Twente in 2001 and 2003 respectively. He is currently working toward the PhD degree in electronic engineering at the University of Twente. During 2003 he visited Integrated Transceivers Group of Natlab, Philips Research Labs., Eindhoven, The Netherlands to carry out his master thesis assignment on high speed, low power frequency dividers in

submicron CMOS technologies. His current research interests are on CMOS frequency dividers and power amplifiers for RF applications. Mr. Acar is the recipient of the Philips Funding for Microelectronics Master Program in University of Twente.



Anne Johan Annema received the M.Sc. degree in electrical engineering and the Ph.D. degree from the University of Twente, Enschede, The Netherlands, in 1990 and 1994, respectively. His doctoral work was on the subject of mathematical analyses and electronic implementations of analog neural networks. It was published as a book: Feed-Forward Neural Networks (Boston, MA: Kluwer, 1995).

In 1995, he joined the Semiconductor Device Architecture Department of Philips Research in Eindhoven, The Netherlands, where he worked on a number of physics-electronics-related projects. In 1997, he joined the Mixed-Signal Circuits and Systems Department at Philips NatLab, where he worked on a number of electronics-physics-related projects ranging from low-power low-voltage circuits, fundamental limits on analog circuits in conjunction with process technologies, high-voltage in baseline CMOS to feasibility research of future CMOS processes for analog circuits.

His current research interest is in physics, analog and mixed-signal electronics, and deep-submicrometer technologies and their joint feasibility aspects. Since June 1 2000 he is with the IC-Design group in the department of Electrical Engineering at the University of Twente, Enschede, The Netherlands. He is also part-time consultant in industry and in 2001 he co-founded Chip Design Works. Anne-Johan is the recipient of the 2003 and 2006 Opel (educational award).